Int. J. Mech. Sci. Vol. 34, No. 7, pp. 563–573, 1992
Printed in Great Britain.

0020–7403/92 $5.00 + .00

POWER-LAW CREEP OF POWDER BONDED BY ISOLATED CONTACTS

L. T. KUHN† and R. M. MCMEEKING‡
†Department of Materials and ‡Department of Mechanical Engineering, University of California, Santa Barbara, CA 93106, U.S.A.

(*Received* 27 *September* 1991)

Abstract—The deformation of powder due to power-law creep near the interparticle contacts is modeled. It is assumed that the plastic dissipation is dominated by the rate of approach of neighboring particles and that the effect of tangential motion can be neglected. To characterize the creep law, the macroscopic strain rate in the powder aggregate is specified and the energy dissipated in power-law creep is computed. This work rate is used in a potential to determine the macroscopic creep parameters. The effective macroscopic shear and dilatational creep properties resulting from this model depend on the relative density of the powder. The creep rates are infinite at random close-packed density. A feature of the creep law is a high sensitivity to changes in deviatoric stress when the stress state is nearly hydrostatic and the creep exponent is high.

INTRODUCTION

In hot isostatic pressing (HIPing) of metal powders, deformation can occur by power-law creep [1]. When loose powder is HIPed, powder deformation occurs by a flattening of the initial point contacts. When this occurs at high temperature, interdiffusion usually takes place quickly between particles so that they readily become bonded together [2]. This stage of HIPing is known as stage I [2] and lasts until the interconnected network of porosity in the powder is broken up into small isolated voids by the pressing of particles. This paper concerns stage I of HIPing.

The macroscopic state of stress in the powder during HIPing is nominally hydrostatic pressure. However, the shielding effect of a container can lead to the powder experiencing unequal macroscopic principal stresses [3, 4]. The container can also cause the deformation to involve a change of shape of the powder aggregate in addition to the consolidation [5]. This effect can also be caused by non-uniform temperature in the powder giving rise to hard and soft regions within the compact [6]. In addition, when powder is consolidated around fibers or other large, hard reinforcements, heterogeneous stress fields arise having a deviatoric component. For all these situations, it is important to have constitutive models to allow the prediction of shape change in powder consolidation. These will be useful for modeling the final shape in the HIPing of complex components and the optimum HIP, pressure or extrusion cycles necessary to consolidate the matrices of composite materials around the reinforcements. It is the purpose of this paper to develop such a constitutive model for stage I power-law creep of bonded powder aggregates.

Helle *et al.* [1] have developed a constitutive model for purely hydrostatic macroscopic stress in the powder aggregate. This stress state leads to a shape-preserving consolidation of the powder. A micromechanical analysis was used by Helle *et al.* [1] to develop their model and we shall make use of their approach to generalize their constitutive law. Other constitutive laws that have been proposed for power-law creep, such as that of Abouaf and Chenot [7], generally are based on a phenomenological approach involving disposable functions whose form is determined by experiment. It is worth noting that micromechanical constitutive models for stage I have been developed for situations where plastic yielding [8] and creep by diffusion [9] control the powder deformation.

POWDER DENSITY, STRESS AND DEFORMATION

An aggregate of powder particles like that shown in Fig. 1 will be considered. The powder particles will be assumed to be initially spherical and monosized. They occupy the fraction

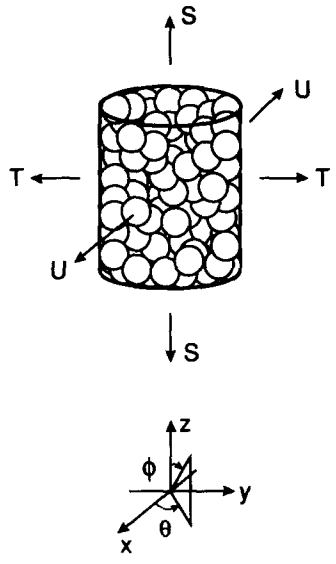

FIG. 1. A volume, V, of the powder aggregate subject to a macroscopic state of stress. A coordinate system is shown also.

D of the total volume V of the powder aggregate with the remaining space being the interstices. The parameter D is known as the relative density, being 1 when the material is fully dense. Within the volume V, the powder packing is statistically random. Thus the macroscopic properties of the aggregate are homogeneous and isotropic. In random close packing the particles make point contact with each other and the interstices are smaller than the particle size so that it is impossible to place another particle in the aggregate without deformation or particle rearrangement. Random close packing of monosized spheres occurs at $D = D_0 \simeq 0.64$. The processing of powder to achieve random close packing is called stage 0 [1] and is not of concern in this paper. The density is taken to be such that $D \geqslant D_0$, but limited to a value which is below the transition to stage II. This is known to occur around $D = 0.9$ [2].

A macroscopic stress Σ is applied to the aggregate of powder at a relative density of D_0 or higher. The principal values of this stress in a Cartesian coordinate system are S, T and U as shown in Fig. 1. As well as any possible inelastic deformation these stresses will cause elastic deformation, leading to Hertzian contact behavior between particles. However, in our treatment we will neglect elasticity, treating the particles as rigid but capable of power-law creep. In response to the applied stress (or vice versa), the powder aggregate will creep with a macroscopic strain rate $\dot{\mathbf{E}}$. Both Σ and $\dot{\mathbf{E}}$ will be treated as uniform in the volume V of interest due to the macroscopic homogeneity of the powder. However, locally within each particle, an inhomogeneous deformation will occur due to the motion of the bonded particles.

The actual motion of each particle during creep will depend on its position within the aggregate, the packing of the particles, the macroscopic strain rate and the creep properties of the material in a complicated way. The particle motion can only be determined properly by analysis of the stresses across particle contacts in conjunction with the macroscopic strain rate and a realization of a macroscopically homogeneous isotropic aggregate. Such a task is formidable and thus well beyond the scope of our paper. Instead, we will develop an approximate model in which the particle centers are assumed to move compatibly with the macroscopic strain rate. This approach was used also by Fleck *et al.* [8] and McMeeking and Kuhn [9]. In consequence, the model constitutive law which results will have bounding properties on the true behavior [10]. According to our assumptions, the motion of a particle with center at $\mathbf{x}$ is such that the velocity of the particle center is

$$v_i = \dot{E}_{ij} x_j. \tag{1}$$

Note that a macroscopic spin rate is omitted, being irrelevant to our considerations. We focus on pairs of neighboring particles for which the difference in center velocity is $\Delta \mathbf{v}$ (see Fig. 2). When the origin of the Cartesian system is placed arbitrarily at the center of one of the particles, as shown in Fig. 3, $\Delta \mathbf{v}$ and $\mathbf{v}$ are equal for the neighboring particle. Thus $\Delta \mathbf{v}$ for that particle can be computed from Eqn (1).

STRESS AND CREEP DISSIPATION AT A BOND BETWEEN PARTICLES

The relative motion of neighboring particles will cause local deformations in the particles for which the local strain rate is $\dot{\varepsilon}$. This strain rate is related to the local stress $\boldsymbol{\sigma}$ by

$$\dot{\varepsilon}_{ij} = \tfrac{3}{2}\dot{\varepsilon}_0(\bar{\sigma}/\sigma_0)^n \sigma'_{ij}/\bar{\sigma} \tag{2}$$

where $\dot{\varepsilon}_0$, σ_0 and n are material parameters, $\boldsymbol{\sigma}'$ is the deviatoric part of $\boldsymbol{\sigma}$ such that

$$\sigma'_{ij} = \sigma_{ij} - \tfrac{1}{3}\sigma_{kk}\delta_{ij} \tag{3}$$

and $\bar{\sigma}$ is the tensile equivalent effective stress

$$\bar{\sigma} = \sqrt{\tfrac{3}{2}\sigma'_{ij}\sigma'_{ij}}. \tag{4}$$

Given that $\Delta \mathbf{v}$ is established for each particle pair, it is necessary to determine the average stress which results across the bond line between the two. For arbitrary combinations of the differences in normal velocity Δv_n and tangential velocity Δv_t, the solution for the average normal stress σ_n and the average tangential stress σ_t (see Fig. 2) is complex for non-linear material and requires numerical analysis. However, Ashby and co-workers [1, 11, 12], using a dimensional argument in Arzt *et al.* [12], developed a model for the relationship between the normal velocity component and the normal average stress when $\Delta v_t = 0$. This has the form

$$\sigma_n = 3\sigma_0\left(\frac{16\Delta v_n}{9\pi\dot{\varepsilon}_0}\sqrt{\frac{\pi}{a}}\right)^{1/n} \tag{5}$$

where a is the area of the bond surface between the two particles. The result applies most precisely when the bond area is very small compared to the total surface area of a single particle. Thus it is most appropriate when the relative density in the powder aggregate is just greater than D_0. However, for purely isostatic deformation, Ashby and co-workers [1, 2] use this model throughout for stage I. Equation (5) is a particular case with $\Delta v_t = 0$ of a more general expression of the form

$$\sigma_n = \sigma_n(\Delta v_n, \Delta v_t). \tag{6}$$

An equivalent result

$$\sigma_t = \sigma_t(\Delta v_n, \Delta v_t) \tag{7}$$

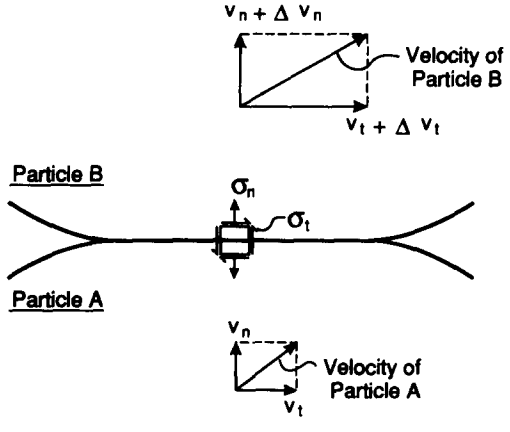

FIG. 2. A particle contact showing the velocity discontinuities and the interface stresses.

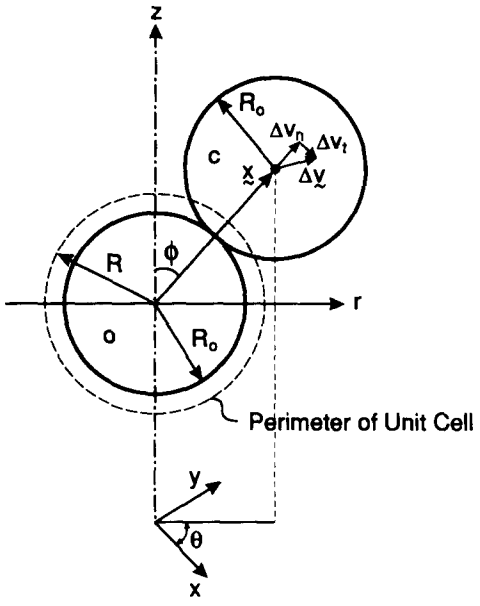

FIG. 3. A pair of particles showing the single unit cell.

can also be stated. As noted above, forms for Eqns (6) and (7) can be determined by numerical analysis.

Instead of pursuing numerical solutions, we will make the following approximation, namely that σ_n is given by Eqn (5) and σ_t is negligible and thus taken to be zero. This is equivalent to an assumption that the creep dissipation rate due to the normal velocity difference is much greater than the dissipation rate due to the tangential velocity difference. Such a situation has been found to prevail in certain circumstances in perfect plasticity [8]. It should be noted that perfect plasticity with a von Mises yield criterion is governed by equations obtained by letting the creep exponent n approach infinity. Thus for high values of n, perhaps 5 and above, the assumption that Eqn (5) always prevails with σ_t negligible can be justified with qualifications. The circumstance for which the assumption cannot be justified is where $\Delta v_n \ll \Delta v_t$, in which case the dissipation due to the tangential velocity difference would dominate. However, in any deformation of a representative powder aggregate, including purely deviatoric strain rate, not all particles are simply sliding by one another [13]. In fact the total number of interparticle contacts for which $\Delta v_n \ll \Delta v_t$ is relatively small compared to the total. Furthermore, because of plastic constraint [8], the creep dissipation rate associated with the contacts for which $\Delta v_n \ll \Delta v_t$ will be swamped by the total dissipation rate associated with all other contacts. Thus, as far as the plastic work rate for high values of n is concerned, the total in a powder aggregate can be estimated quite well by use of Eqn (5) to give σ_n associated with $\sigma_t = 0$. In that case, the creep dissipation rate per unit area of contact for any particle pair bonded together is given by

$$\sigma_n \Delta v_n = 3\sigma_0 \left(\frac{16}{9\pi \dot{\varepsilon}_0} \sqrt{\frac{\pi}{a}} \right)^{1/n} |\Delta v_n|^{1/n+1} \tag{8}$$

where the absolute value of Δv_n ensures that the dissipation rate is always positive. The result for perfect plasticity is obtained by taking the limit as $n \to \infty$ giving $3\sigma_0 |\Delta v_n|$. In that case σ_0 is defined to be the yield stress in uniaxial tension and the coefficient 3 denotes the Prandtl punch level of constraint which would prevail for contacts very small compared to particle size [1, 8].

CREEP DISSIPATION RATE FOR THE POWDER AGGREGATE

The total creep dissipation rate for the powder aggregate can be calculated from Eqn (8) by integrating it over all contacts between particles. However, every bond in the powder

aggregate can be represented with respect to the particle pair shown in Fig. 3. That is, to compute Δv_n for a particular contact, the origin can be placed at the center of one of the two particles. Consider a strain rate axisymmetric about the z-axis and define the parameters

$$\dot{H} = \dot{E}_{kk} \tag{9}$$

and

$$\dot{E} = \tfrac{2}{3}(\dot{E}_{zz} - \dot{E}_{xx}). \tag{10}$$

The normal component of the velocity difference for the two particles in Fig. 3 is then given by

$$\Delta v_n = R_0[\dot{E}(3\cos^2\phi - 1) + 2\dot{H}/3]. \tag{11}$$

The result in Eqn (11) can be substituted into Eqn (8) to give the creep dissipation rate per unit area of the bonded contact at orientation ϕ.

In the powder aggregate, due to isotropy, the probability of finding a neighboring particle at any orientation with respect to a given particle is equal. Furthermore, Helle *et al.* [1], based on the work of Arzt [14] and Fischmeister and Arzt [15], have shown that for spherical monosized particles packed isotropically the fraction of a particle surface bonded to a neighbor is

$$f = D(D - D_0)/(1 - D_0). \tag{12}$$

This relationship indicates that when the relative density is D_0 (random close packing) the bonded area is zero (point contact) and at theoretical density ($D = 1$) the whole surface of the particle is bonded to neighbors. As well as giving these sensible limits, the expression has been found to model experimental data quite accurately at densities below 0.9 [14, 15]. Since we are concerned only with stage I ($D \lesssim 0.9$), this is satisfactory. In addition, Helle *et al.* [1] determined that the area of a single bonded contact is

$$a = \frac{\pi}{3}\left(\frac{D - D_0}{1 - D_0}\right) R_0^2. \tag{13}$$

Using the pair in Fig. 3 as representative of any neighboring particles, the total creep dissipation per particle can be computed by integrating the creep dissipation per unit area of bonded contact [Eqn (8)] over the particle surface. This result must be multiplied by the fraction of the area in contact with neighbors [Eqn (10)] and divided by 2 to account for the fact that the dissipation is shared by two particles. By dividing this in turn by the volume occupied by a unit cell containing one particle ($\frac{4}{3}\pi R_0^3/D$, see Fig. 3), the creep dissipation rate per unit macroscopic volume can be established. This is

$$W_V = C(\sigma_0/\dot{\varepsilon}_0^{1/n}) \int_0^{\pi} |\dot{E}(3\cos^2\phi - 1) + 2\dot{H}/3|^{1+1/n} \sin\phi \, \mathrm{d}\phi \tag{14}$$

where

$$C = \frac{9}{4}\left(\frac{16\sqrt{3}}{9\pi}\right)^{1/n} D^2 \left(\frac{D - D_0}{1 - D_0}\right)^{1 - 1/2n}.$$

CREEP POTENTIAL

The macroscopic creep rate of the powder aggregate can be expressed in terms of a potential as follows:

$$\dot{E}_{ij} = \partial\Psi/\partial\Sigma_{ij}. \tag{15}$$

Cocks [10] has shown from the convexity of Ψ that

$$\Psi(\Sigma) \geqslant \Sigma_{ij}\dot{E}_{ij} - \frac{n}{n+1} W_V(\dot{\mathbf{E}}) \tag{16}$$

where $\dot{\mathbf{E}}$ is any homogeneous strain rate of the powder aggregate. The inequality arises because W_V is not an exact calculation of the creep dissipation per unit volume due to $\dot{\mathbf{E}}$ in

the powder aggregate but rather is an estimate based on the kinematical assumption that each particle center moves compatibly with $\dot{\mathbf{E}}$. If an exact calculation of W_V could be carried out, then the equality would pertain. In addition, it should be remembered that the dissipation rate due to relative shearing motions of particles has been neglected. This approximation means that in our case the inequality cannot be enforced strictly. However, we shall proceed as if the inequality were truly valid with the expectation that our neglect of the shearing dissipation will not be that significant.

The best lower bound to Ψ for a given Σ can be obtained by maximizing the right-hand side of Eqn (16) with respect to $\dot{\mathbf{E}}$. This leads to

$$\Sigma_{ij} = \frac{n}{n+1}\frac{\partial W_V(\dot{\mathbf{E}})}{\partial \dot{E}_{ij}}. \tag{17}$$

Since we are restricting ourselves to axisymmetric states, W_V is a function of strain rate only through $\dot{H}$ and $\dot{E}$ and Eqn (17) gives

$$\Sigma_m = \frac{n}{n+1}\frac{\partial W_V(\dot{H}, \dot{E})}{\partial \dot{H}} \tag{18}$$

and

$$\Sigma = \frac{n}{n+1}\frac{\partial W_V(\dot{H}, \dot{E})}{\partial \dot{E}} \tag{19}$$

where $\Sigma_m = \Sigma_{kk}/3$ is the mean stress and

$$\Sigma = \Sigma_{zz} - \Sigma_{xx} = S - T \tag{20}$$

where $T = U$ (see Fig. 1). Differentiation of Eqn (14) then gives

$$\Sigma_m = \frac{C\sigma_0}{\dot{\varepsilon}_0^{1/n}}\int_0^{\pi} |\dot{E}(3\cos^2\phi - 1) + 2\dot{H}/3|^{(1-n)/n}[\dot{E}(3\cos^2\phi - 1) + 2\dot{H}/3]\frac{2}{3}\sin\phi\,d\phi \tag{21}$$

and

$$\Sigma = \frac{C\sigma_0}{\dot{\varepsilon}_0^{1/n}}\int_0^{\pi} |\dot{E}(3\cos^2\phi - 1) + 2\dot{H}/3|^{(1-n)/n}[\dot{E}(3\cos^2\phi - 1) + 2\dot{H}/3](3\cos^2\phi - 1)\sin\phi\,d\phi. \tag{22}$$

These expressions can be regarded as constitutive laws giving Σ and Σ_m in terms of $\dot{E}$ and $\dot{H}$. However, we proceed to compute the associated (best) bound on Ψ from Eqn (16) and call it $\bar{\Psi}$. At this stage $\bar{\Psi}$ can only be expressed in terms of $\dot{H}$ and $\dot{E}$ as

$$\bar{\Psi} = \Sigma_m\dot{H} + \Sigma\dot{E} - \frac{n}{n+1}W_V(\dot{H}, \dot{E})$$

$$= \frac{C\sigma_0}{\dot{\varepsilon}_0^{1/n}(1+n)}\int_0^{\pi} |\dot{E}(3\cos^2\phi - 1) + 2\dot{H}/3|^{1+1/n}\sin\phi\,d\phi \tag{23}$$

a result which arises because of the homogeneity of W_V in terms of $\dot{H}$ and $\dot{E}$. From now on Eqn (23) will be regarded as an estimate for the creep potential Ψ.

The estimate for Ψ can be portrayed graphically as contours in stress space for which $\bar{\Psi}$ is constant. For convenience, we can consider the situation where $\bar{\Psi}(n+1)/C\sigma_0\dot{\varepsilon}_0$ is equal to $2(2/3)^{(n+1)/n}$. The procedure is to iterate to find values for $\dot{E}/\dot{\varepsilon}_0$ and $\dot{H}/\dot{\varepsilon}_0$ together which render $\bar{\Psi}(n+1)/C\sigma_0\dot{\varepsilon}_0$ equal to that value. These values for $\dot{E}/\dot{\varepsilon}_0$ and $\dot{H}/\dot{\varepsilon}_0$ are then inserted into Eqns (21) and (22) to give results for $\Sigma_m/\sigma_0 C$ and $\Sigma/\sigma_0 C$ which are plotted against each other in Fig. 4. The resulting contours are level lines of the estimate for the potential Ψ.

APPROXIMATE FORM FOR THE CREEP POTENTIAL

It is helpful for application of the constitutive law to represent the potential Ψ in terms of elementary functions. This can be done by curve fitting to the contours shown in Fig. 4.

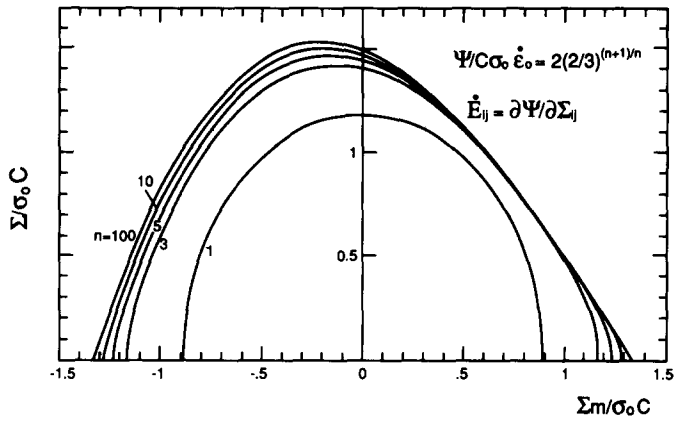

FIG. 4. Contours in stress space for which the creep potential estimate $\bar{\Psi}$ is constant. Σ_m is the mean stress and Σ is an effective measure of the deviatoric stress.

However, it should be noted that the shapes of the curves are suspect when Σ_m is small compared to Σ because then the neglect of the dissipation due to particles shearing past each other is most significant. Furthermore, for modeling powder consolidation, the constitutive law when Σ_m is large compared to Σ is of most interest. Thus we focus on fitting curves to the contour segments near the Σ_m axis in Fig. 4. Another difficulty is that the contours in Fig. 4 are not symmetric and have different shapes in each quadrant. This is related to the feature that the contours represent only axisymmetric states of stress. The non-symmetry indicates that the creep potential depends on all three invariants of stress. A simplification can be made through the assumption that an approximate potential representation can be constructed with dependence only on the first (Σ_m) and second ($\Sigma^2/3$) invariants of stress. This will be done by fitting to the curves in the first quadrant ($\Sigma_m, \Sigma \geqslant 0$) of Fig. 4. This is exactly equivalent to fitting to the curves in the third quadrant ($\Sigma_m, \Sigma \leqslant 0$).

It is found that the contours near the Σ_m axis in the first quadrant of Fig. 4 can be fitted with

$$\left(\frac{|\Sigma_m|}{\Sigma_m^0}\right)^{(n+1)/n} + \left(\frac{2\Sigma_e}{3\Sigma_m^0}\right)^{(n+1)/n} = 1 \tag{24}$$

where $\Sigma_m^0 = 2(2/3)^{1+1/n}\sigma_0 C$ and $\Sigma_e = |\Sigma|$. An interesting feature is that when $n = 1$, the shape is an ellipse. When n is very large, the curve is composed of nearly straight lines connected by regions of high curvature near the Σ_m and Σ_e axes.

Use of Eqns (21), (23) and (24) leads to the result

$$\Psi = \frac{\dot{\varepsilon}_0\sigma_0}{n+1}\frac{27\pi}{16\sqrt{3}}\left(\frac{D-D_0}{1-D_0}\right)^{1/2}\left\{\frac{(1-D_0)}{3D^2(D-D_0)}\left[\left(\frac{|\Sigma_m|}{\sigma_0}\right)^{(n+1)/n} + \left(\frac{2\Sigma_e}{3\sigma_0}\right)^{(n+1)/n}\right]\right\}^n. \tag{25}$$

Differentiation according to Eqn (15) gives the strain rate

$$\dot{E}_{ij} = \dot{\varepsilon}_0\frac{27\pi}{16\sqrt{3}}\left(\frac{D-D_0}{1-D_0}\right)^{1/2}\left[\frac{(1-D_0)}{3D^2(D-D_0)}\right]^n\left[\left(\frac{|\Sigma_m|}{\sigma_0}\right)^{(n+1)/n} + \left(\frac{2\Sigma_e}{3\sigma_0}\right)^{(n+1)/n}\right]^{n-1}$$
$$\times\left[\left(\frac{|\Sigma_m|}{\sigma_0}\right)^{1/n}(\text{sign }\Sigma_m)\frac{1}{3}\delta_{ij} + \left(\frac{2\Sigma_e}{3\sigma_0}\right)^{1/n}\frac{\Sigma'_{ij}}{\Sigma_e}\right] \tag{26}$$

where sign Σ_m is $+1$ when Σ_m is positive and equal to -1 when Σ_m is negative. In the case of purely hydrostatic pressure, Eqn (26) gives

$$\dot{E}_{ij} = -\dot{\varepsilon}_0\frac{27\pi}{16\sqrt{3}}\left(\frac{D-D_0}{1-D_0}\right)^{1/2}\left[\frac{(1-D_0)}{3D^2(D-D_0)}\right]^n\left(\frac{\Sigma_m}{\sigma_0}\right)^n\frac{1}{3}\delta_{ij} \tag{27}$$

which shows that the strain rate is a pure volume reduction. Given that $\dot{E}_{kk} = -\dot{D}/D$, Eqn (27) is identical to the purely isostatic result of Ashby in the form stated in [2]. In more general terms, when Σ_m is positive the dilatational strain rate $\dot{H}$ is given by

$$\dot{H} = \dot{\varepsilon}_0 \frac{27\pi}{16\sqrt{3}} \left(\frac{D - D_0}{1 - D_0}\right)^{1/2} \left[\frac{(1 - D_0)}{3D^2(D - D_0)}\right]^n \left[\left(\frac{\Sigma_m}{\sigma_0}\right)^{(n+1)/n} + \left(\frac{2\Sigma_e}{3\sigma_0}\right)^{(n+1)/n}\right]^{n-1} \left(\frac{\Sigma_m}{\sigma_0}\right)^{1/n} \tag{28}$$

and the effective strain rate

$$\dot{E}_e = \sqrt{\frac{2}{3}\dot{E}'_{ij}\dot{E}'_{ij}}$$

$$= \frac{27\pi}{16\sqrt{3}} \left(\frac{D - D_0}{1 - D_0}\right)^{1/2} \left[\frac{(1 - D_0)}{3D^2(D - D_0)}\right]^n \left[\left(\frac{\Sigma_m}{\sigma_0}\right)^{(n+1)/n} + \left(\frac{2\Sigma_e}{3\sigma_0}\right)^{(n+1)/n}\right]^{n-1} \frac{2}{3}\left(\frac{2\Sigma_e}{3\sigma_0}\right)^{1/n} \tag{29}$$

FEATURES OF THE CREEP LAW

The relative density has a strong effect on the creep rate of the powder aggregate. The creep rate is proportional to $(D - D_0)^{1/2-n}$ so that when $D = D_0$ at random close packing the creep rate is infinite. Physically, this is due to the fact that at random close packing of rigid spheres there is point bonding and when stress is applied the stress transmitted through the bonds is infinite. This leads to an infinite creep strain rate. A proper treatment of elastic effects would change this feature somewhat, especially in compression where Hertzian contact would allow flattening of the contacts prior to creep. However, even with elastic effects, the creep rate of the aggregate will be very high when the relative density is near the random close packed level. As the relative density of the aggregate increases, the creep rate drops in proportion to $(D - D_0)^{1/2-n}$ due to the enlargement of the bonded area between neighboring particles.

However, the constitutive law Eqn (26) is designed to represent best the behavior at low relative densities. At higher relative densities a variety of features make the law less likely to be accurate. For example, the modeling of the creep rate between neighboring particles is largely based on the behavior of nearly spherical particles which are bonded together by necks with a tiny area. As the relative density increases, the area of an individual bonded contact will represent a sizeable fraction of the surface area of a particle. In this situation, the creep zone adjacent to a particular contact will interact quite strongly with the creep zone of a neighboring contact. This effect is neglected in our treatment. Thus we expect the creep law Eqn (26) to be less appropriate at higher relative densities. As stated before, we intend the law to be used only for $D \leqslant 0.9$ in any case but it may well have substantial inaccuracies associated with it at that level of relative density.

It is worthwhile considering the sensitivity of the strain rates in Eqn (26) in terms of the stress. This is most readily achieved through the ratio $\dot{E}_e/\dot{H}$ which from Eqns (28) and (29) is

$$\dot{E}_e/\dot{H} = (2/3)(2\Sigma_e/3\Sigma_m)^{1/n} \tag{30}$$

given positive Σ_m. When $n = 1$, $\dot{E}_e/\dot{H}$ is linearly dependent on Σ_e/Σ_m reflecting the elliptical shape of the creep potential in that case. When n is infinite, giving rise to perfect plasticity, $\dot{E}_e/\dot{H}$ is independent of the stress ratio, which occurs because then the potential is a straight line. However, in perfect plasticity there is a vertex on the yield surface when $\Sigma_e = 0$ and the strain rate is non-unique when the stress is purely hydrostatic [8]. This can be interpreted to mean that in perfect plasticity the strain rate is very sensitive to the addition of a small amount of effective stress, Σ_e, to a state of pure hydrostatic stress. When the stress is non-hydrostatic, the strain rate is insensitive to changes in the stress ratio as long as Σ_e remains non-zero. A similar situation prevails when n is not infinity but merely large, say above 5. In that case, $\dot{E}_e/\dot{H}$ varies rapidly with Σ_e/Σ_m when the stress state is nearly hydrostatic, i.e. the latter ratio is small compared to unity (taking Σ_m to be positive). When Σ_e/Σ_m is larger than 1, $\dot{E}_e/\dot{H}$ is relatively unaffected by changes in the stress ratio. Since the

tangent of the normal to contours in Fig. 4 is $\dot{E}_e/\dot{H}$, this behavior reflects the high degrees of curvature near the hydrostatic stress axis in these contours and their relative straightness elsewhere. As n approaches ∞, the highly curved region of the contours becomes almost a vertex.

Finally, the uniaxial stress case is useful for comparison with experiment. In uniaxial tension with $\Sigma_{zz} = S$ (taken to be positive) and other stress components equal to zero, Eqn (26) predicts that

$$\dot{E}_{zz} = \dot{\varepsilon}_0 \frac{9\pi}{16\sqrt{3}} \left(\frac{D - D_0}{1 - D_0}\right)^{1/2} \left[\frac{(1 - D_0)}{3D^2(D - D_0)}\right]^n (1 + 2^{(n+1)/n})^n \left(\frac{S}{3\sigma_0}\right)^n \tag{31}$$

and

$$\dot{E}_{xx} = \dot{E}_{yy} = \dot{\varepsilon}_0 \frac{9\pi}{16\sqrt{3}} \left(\frac{D - D_0}{1 - D_0}\right)^{1/2} \left[\frac{(1 - D_0)}{3D^2(D - D_0)}\right]^n (1 + 2^{(n+1)/n})^{n-1} (1 - 2^{1/n}) \left(\frac{S}{3\sigma_0}\right)^n. \tag{32}$$

The resulting ratio of strain rates $\dot{E}_{xx}/\dot{E}_{zz}$, which we denote by v, is

$$v = \frac{(1 - 2^{1/n})}{(1 + 2^{(n+1)/n})}. \tag{33}$$

When $n = 1$, the ratio is -0.2 but when n is infinity (perfect plasticity) $v = 0$. That is, in the latter case, uniaxial stress induces a uniaxial strain rate. Similarly, for high values of n, the strain rate will be nearly uniaxial. Even for $n = 2$, the ratio of strain rates is -0.11, showing that the deformation is nearly uniaxial.

COMPARISON WITH OBSERVED BEHAVIOR

The purely isostatic form of the creep law given in Eqn (27) was developed previously by Ashby and co-workers [1, 2] and compared with HIP data by Ashby [2]. There is good agreement between the model and the data for low-carbon steel powder with a 100–125 μm particle size and for alumina. Agreement is reasonable but less good for copper powder, but in that case the material properties used in the calculation may not be the correct ones. Thus, in one special case, the creep law in Eqn (26) is quite reliable.

Casagranda *et al.* [16] have tested alumina powder aggregates in uniaxial compression. These were first sintered to make them coherent. By sintering to different relative densities, they were able to produce a set of initially isotropic powder compacts which were tested at different stresses and temperatures. The data were normalized according to the known properties of fully dense fine grained alumina. The dimensionless group

$$\frac{\dot{\varepsilon} d^2 \mathrm{k}\, T_\mathrm{A} G}{\Omega^{2/3} \delta_\mathrm{b} D_\mathrm{b} \sigma^2}$$

was plotted against relative density as shown in Fig. 5. In the group, $\dot{\varepsilon}$ is the axial compressive strain rate, σ is the compressive axial stress, d is the grain size, k is Boltzmann's constant, T_A is the absolute temperature, G is the shear modulus of alumina, Ω is the atomic volume and $\delta_\mathrm{b} D_\mathrm{b}$ is a grain boundary diffusion parameter. Although diffusion plays a role in the creep process of fine-grained alumina, the creep exponent is 2 and thus a power-law model is called for. The other parameters in the dimensionless group are those that determine the value of $\dot{\varepsilon}_0/\sigma_0^2$ in the creep law. Thus the group is effectively equal to $\xi(\dot{\varepsilon}/\dot{\varepsilon}_0)/(\sigma/\sigma_0)^2$, being only a function of the relative density. This is confirmed by Fig. 5 which portrays data from several different experiments in which some of the parameters in the dimensionless group had different values.

Taking the uniaxial result for $\dot{E}_{zz}$ with $n = 2$ and converting it to compression, we find that Eqn (31) predicts

$$\frac{\dot{\varepsilon}/\dot{\varepsilon}_0}{(\sigma/\sigma_0)^2} = \frac{0.19}{D^4} \left(\frac{1 - D_0}{D - D_0}\right)^{3/2} \tag{34}$$

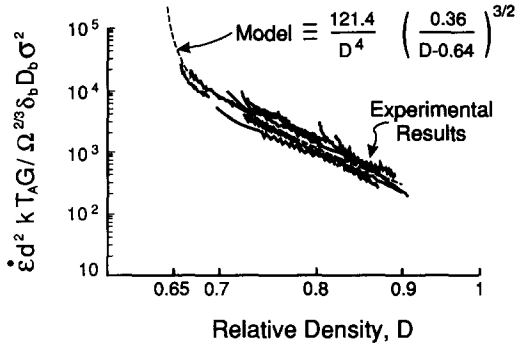

FIG. 5. Comparison of the model with uniaxial compression data for alumina powder.

where $D_0 = 0.64$. In view of uncertainties in the absolute value of various parameters in the dimensionless group, the right-hand side of Eqn (34) has been multiplied by a number (i.e. a value for ξ) to make the prediction at $D = 0.8$ agree with the experimental data in Fig. 5. The result has been plotted in the range $0.65 \leqslant D \leqslant 0.9$. It can be seen that the agreement is excellent, indicating that the behavior is predicted well by the model over the relative density range involved, including the initial rapid densification rate for compacts with D close to 64%.

In addition, the transverse strain rate is predicted well. Casagranda *et al.* [16] found that the strain rate ratio $v = \dot{E}_{xx}/\dot{E}_{zz}$ was -5% to -10% in the relative density range $0.66 \leqslant D \leqslant 0.9$. As noted before, for $n = 2$ our model predicts $v = -11\%$.

DISCUSSION

The constitutive model developed in this paper is based on the neglect of the creep dissipation associated with relative tangential motion of neighboring particles. It has been established by Kuhn [17] that creep potentials based on numerical calculations of the creep dissipation including the effect of tangential motion are little different from those developed in this paper. Thus, we have some confidence in the validity of the approximated creep potential Eqn (25).

The associated constitutive law for the creep behavior of powder aggregates can be used to predict the consolidation of powder around reinforcements such as fully dense ceramic fibers in composite materials. In addition, it can be used in calculations predicting the rate of consolidation in uniaxial pressing of powders and for similar computations involving the hot forging of complex shapes from powder compacts. Another important possibility is the modeling of final shape in forming processes such as HIPing. In relation to these calculations, an interesting feature is the high degree of sensitivity of the deviatoric strain rate to the stress when n is high and the stress is nearly hydrostatic. The corollary of this statement is that the deviatoric stress is relatively insensitive to the strain rate when the stress is nearly hydrostatic. Thus, substantial deviatoric strains can be imposed on a consolidation process whilst the deviatoric stresses remain small compared to the hydrostatic pressure. Thus it is possible that flow around reinforcements, deformation into complex shapes and shape-changing deformations can be achieved, without substantial perturbation of the pressure required to achieve the densification (either up or down) [18, 19]. This could be good (no elevation of the pressure required) or bad (no enhancement of the densification rate due to small amounts of shear, difficult to control shape) depending on the circumstances. However, these comments apply only to stage I with high n and not necessarily to stage I controlled by diffusion [9] or to any deformation in stage II.

CONCLUSIONS

A creep constitutive law for power-law materials has been developed for powder aggregates when the growth or enlargement of bonded contacts controls the deformation. The creep rate

is strongly dependent on the relative density, falling off from infinity as the relative density increases from 64%. The law is valid for a density range from 64% to about 90%.

Dilatation occurs in response to hydrostatic stress and deviatoric strain rates exist when there is deviatoric stress. However, the law shows a non-linear interaction (when $n \neq 1$) between the hydrostatic and deviatoric stresses. When the creep exponent n is high compared to 1, the deviatoric strain rate is highly sensitive to the deviatoric stress when the stress is nearly purely hydrostatic but is insensitive in other circumstances.

The purely hydrostatic version of the creep law agrees well with data for isostatic consolidation of powder. The uniaxial stress form predicts well the behavior of sintered powder aggregates of alumina in compression.

Acknowledgements—This research was supported by the National Science Foundation through grant DMR 8713919 to the University of California, Santa Barbara.

REFERENCES

1. A. S. HELLE, K. E. EASTERLING and M. F. ASHBY, Hot-isostatic pressing diagrams: new developments. *Acta Metall.* **33**, 2163 (1985).
2. M. F. ASBHY, *HIP 6.0 Background Reading*. University of Cambridge Engineering Department, Trumpington St, Cambridge CB2 IPZ, U.K. (1990).
3. H. N. G. WADLEY, R. J. SCHAEFER, A. H. KAHN, M. F. ASHBY, R. B. CLOUGH, Y. GEFFEN and J. J. WLASSICH, Sensing and modelling of the hot isostatic pressing of copper powder. *Acta Metall. Mater.* **39**, 979 (1991).
4. J. XU and R. M. MCMEEKING, An analysis of the effect of the can in an isostatic pressing of copper powder. *Int. J. Mech. Sci.* **34**(2), 167 (1992).
5. M. F. ASHBY, Powder compaction under non-hydrostatic stress states: an initial survey. To be published (1991).
6. W.-B. LI, M. F. ASHBY and K. E. EASTERLING, On densification change and shape change during hot isostatic pressing. *Acta Metall.* **35**, 2831 (1987).
7. M. ABOUAF and J. L. CHENOT, Modelisation numerique de la déformation à chaud de poudres metalliques. *J. Mech. Theoret. Appliq.* **5**, 121 (1986).
8. N. A. FLECK, L. T. KUHN and R. M. MCMEEKING, Yielding of metal powder bonded by isolated contacts. *J. Mech. Phys. Solids* **40** (5), 1139 (1992).
9. R. M. MCMEEKING and L. T. KUHN, A diffusional creep law for powder compacts. To appear in *Acta Metall. Mater.* (1991)
10. A. C. F. COCKS, Inelastic deformation of porous materials. *J. Mech. Phys. Solids* **37**, 693 (1989).
11. D. S. WILKINSON and M. F. ASHBY, Pressure sintering by power law creep. *Acta Metall.* **23**, 1277 (1975).
12. E. ARZT, M. F. ASHBY and K. E. EASTERLING, Practical applications of hot-isostatic pressing diagrams: four case studies. *Metall. Trans. A* **14A**, 211 (1983).
13. G. SUBHASH, S. NEMAT-NASSER, M. M. MEHRABADI and H. M. SHODJA, Experimental investigation of fabric-stress relations in granular materials. *Mech. Mater.* **11**, 87 (1991).
14. E. ARZT, The influence of an increasing particle coordination on the densification of spherical powders. *Acta Metall.* **30**, 1883 (1982).
15. H. F. FISCHMEISTER and E. ARZT, Densification of powders by particle deformation. *Powder Metall.* **26**, 82 (1983).
16. A. CASAGRANDA, F. W. ZOK and A. G. EVANS, The densification of alumina and alumina matrix composites. To be published (1991).
17. L. T. KUHN, Constitutive laws for the deformation of bonded powder aggregates. Ph.D. Dissertation, Materials Department, University of California, Santa Barbara (1991).
18. R. M. MCMEEKING, The consolidation of powder around a fiber to form a matrix. *Mech. Mater.* **12**, 85 (1991).
19. R. M. MCMEEKING, The analysis of shape change during isostatic pressing. *Int. J. Mech. Sci.* **34** (1), 53 (1992).